

## RAM PRESSURE STRIPPING IN CLUSTERS AND GROUPS

J.A. HESTER<sup>1</sup>

*Draft version September 10, 2018*

### ABSTRACT

Ram pressure stripping is an important process in the evolution of both dwarf galaxies and large spirals. Large spirals are severely stripped in rich clusters and may be mildly stripped in groups. Dwarf galaxies can be severely stripped in both clusters and groups. A model is developed that describes the stripping of a satellite galaxy's outer H I disk and hot galactic halo. The model can be applied to a wide range of environments and satellite galaxy masses. Whether ram pressure stripping of the outer disk or hot galactic halo occurs is found to depend primarily on the ratio of the satellite galaxy mass to the mass of the host group or cluster. How the effectiveness of ram pressure stripping depends on the density of the inter-group gas, the dark matter halo concentrations, and the scale lengths and masses of the satellite components is explored. The predictions of the model are shown to be well matched to H I observations of spirals in a sample of nearby clusters. The model is used to predict the range of H I gas fractions a satellite of mass  $M_{v,sat}$  can lose orbiting in a cluster of mass  $M_{v,gr}$ .

*Subject headings:* galaxies: evolution — galaxies:clusters:general — galaxies:dwarf

### 1. INTRODUCTION

Ram pressure stripping was first proposed by Gunn & Gott (1972) to explain the observed absence of gas-rich galaxies in clusters. They noted that galaxies falling into clusters feel an intracluster medium (ICM) wind. If this wind can overcome the gravitational attraction between the stellar and gas disks, then the gas disk will be blown away. They introduced a simple analytical condition to determine when gas is lost:

$$\rho_{ICM} v_{sat}^2 < 2\pi G \sigma_* \sigma_{gas}. \quad (1)$$

The right-hand side,  $2\pi G \sigma_* \sigma_{gas}$ , is a gravitational restoring pressure,  $\rho_{ICM}$  is the density of the ICM, and  $v_{sat}$  is the orbital speed of the satellite galaxy. Using this condition they concluded that spirals should lose their gas disks when they pass through the centers of clusters.

Galaxies near cluster centers have earlier type morphologies, are redder, and form fewer stars than galaxies in the field of similar luminosity (Gomez et al. 2003; Goto et al. 2003; Hogg et al. 2003, 2004). Stripped galaxies have low H I masses for their size and morphology. Such H I deficiency correlates with lower star formation rates (SFRs) (Gavazzi et al. 2006), and lowered SFRs lead to redder colors. Therefore, ram pressure stripping, in conjunction with processes like harassment that can alter the structure of a galaxy, may play a role in transforming galaxy morphologies.

Several sets of observations indicate that stripping occurs to spirals in clusters. Giovanelli & Haynes (1983) define a deficiency parameter that compares a galaxy's observed H I mass to the expected H I mass in a field galaxy with the same morphology and optical size. Galaxies in Virgo, (Giovanelli & Haynes 1983), Coma, (Bravo-Alfaro et al. 2000), and other nearby clusters, (Solanes et al. 2001) are observed to be H I deficient. Solanes et al. (2001) observe that the average deficiency increases with decreasing distance to the clusters' centers

and that deficient galaxies have, on average, more eccentric orbits. Cayatte et al. (1994) observe indications of stripping in the H I distributions of individual galaxies in the Virgo cluster. Compared to an average profile for a field galaxy of similar morphology and optical extent, these galaxies have normal gas densities in their inner disks but are sharply truncated. More detailed observations of several Virgo spirals have since been carried out. NGC 4522 is observed to have an undisturbed optical disk, a severely truncated H I disk, and extra planar H $\alpha$  and H I on one side of the disk (Kenney & Koopman 1999; Kenney et al. 2004b). IC 3392, NGC 4402, NGC 4419, and NGC 4388 all have a truncated H I disk, and the first three have extraplanar H I (Kenney et al. 2004a). NGC 4569 has a truncated H I disk and extra planar H $\alpha$  (Kenney et al. 2004a). Observing asymmetric, extraplanar gas in combination with an undisturbed optical disk is a strong indication that the galaxy's gas is interacting with the ICM.

Detailed simulations of ram pressure stripping confirm that spirals in clusters should be stripped. For some simulations the final radii of the galaxies are compared to the predictions of the Gunn and Gott condition. In addition, the morphologies of simulated galaxies have been compared to observations of spirals in Virgo. Simulations by Abadi et al. (1999) show that galaxies in a face-on wind are stripped to radii near those predicted by the Gunn and Gott condition, but galaxies in an edge-on wind are only mildly stripped. In contrast, other simulations show a two-step stripping process that strips galaxies at all inclination angles. Ram pressure stripping first quickly strips gas from the outer disk, and then the remaining disk is slowly viscously stripped (Marcolini et al. 2003; Quilis et al. 2000; Roediger & Hensler 2005; Schulz & Struck 2001). Marcolini et al. (2003) point out that, unlike ram pressure stripping, viscous stripping is more effective in an edge-on wind. They find that the final radii of the face-on galaxies match those predicted using the Gunn and Gott condition and that edge-on galaxies are stripped

Electronic address: jhester@princeton.edu

<sup>1</sup> Jadwin Hall, Princeton University, Princeton, NJ, 08540

to slightly larger radii. Roediger & Hensler (2005) run a series of simulations to test the dependence of the stripping radius on the speed of the ICM wind, the mach number, and the vertical structure of the gas disk. They find that the most important parameters are the ram pressure and surface density of the gas disk and that the effects of varying the mach number and vertical structure are minor. They find that the original Gunn and Gott condition does a fair job predicting the stripping radius. However, when they use an adjusted ram pressure, they find that using the thermodynamic pressure in the central plane of the disk more accurately predicts the stripping radius.

Simulations of ram pressure stripping can also match the range of morphologies of stripped galaxies. Vollmer et al. (2000, 2004) track the density, velocity, and velocity dispersion of a simulated galaxy's cold disk gas. In NGC 4522, the kinetically continuous extraplanar gas matches simulations of a galaxy that is currently being stripped. However, the gas in NGC 4569 is less pronounced, not kinetically continuous with the disk gas, and has a large velocity dispersion, more like simulations of a galaxy that has been stripped in the past. In their simulations Schulz & Struck (2001) observe a process they term "annealing". The ICM wind compresses the gas disk and triggers the formation of large spiral arms. The interaction of these arms with the wind leads to the contraction of the galaxy and the formation of a dense truncated gas disk. A burst of star formation may occur at the edge of the truncated disk. A ring of star formation is seen at the truncation radius of the disk in IC 3392.

Some groups have studied stripping in groups and cluster outskirts where the ram pressure is lower than in cluster centers. While simulations and observations both support the idea that large spirals in clusters are stripped of their H I disks, it is not clear that stripping occurs in poorer environments. Two types of stripping may occur in groups. The ram pressure in groups is lower than in clusters. However, dwarf galaxies have lower masses than large spirals and therefore lower restoring pressures, and dwarf galaxies may be stripped of most of their H I. In addition, large spirals have restoring pressures that decrease with radius and may be stripped of their outer disks. Marcolini et al. (2003) run simulations of dwarf-like galaxies in winds typical of the ram pressure in groups and find that the simulated dwarfs are stripped. The Roediger & Hensler (2005) simulations include runs with low ram pressure. Their large and medium-sized model spirals are stripped of some of their outer H I in these runs. The observational evidence for stripping in low-mass systems is circumstantial. The gas content and star formation histories of Local Group dwarfs correlate with their distances from the dominant spirals (Blitz & Robishaw 2000; Grebel 2002).

This project aims to use the clear observations of stripping in clusters to predict when stripping occurs in groups. This is done by examining how the ram and restoring pressures depend on the masses of the cluster or group and the satellite galaxy. Two ways in which the masses of the host system and satellite galaxy affect the ram and restoring pressures are identified. Satellites' orbital speeds are set by the depth of the cluster's potential, and the restoring force on the gas disk is determined by

the depth of the satellite's potential. In addition, both cluster and galaxy morphologies change with mass. A model is developed and used to study both types of mass dependence. This is done in the following steps.

In the next section a model for the mass and gas distributions is presented both in terms of physical parameters and in terms of scale-free parameters. In section 3 the dependence of ram pressure stripping on the masses of the satellite and cluster is presented assuming that the scale-free parameters are constant. In section 4 the dependence of the scale-free parameters on the masses of the satellite and cluster and the sensitivity of the model to these changes are explored. In section 5 the results are discussed and the model is compared to observations of stripping. Section 6 concludes.

## 2. THE MODEL

The analytical model of ram pressure stripping developed here uses the Gunn and Gott condition to predict the extent to which galaxies are stripped. This condition is based on a simplified picture of stripping that ignores the details of the hydrodynamical processes and balances forces on large scales. However, simulations of galaxies that are stripped by a face-on wind result in stripping radii that match the predictions of the Gunn and Gott condition (Abadi et al. 1999; Marcolini et al. 2003; Roediger & Hensler 2005). In the simulations galaxies in an edge on wind are eventually viscously stripped to radii similar to those of face-on, ram pressure stripped galaxies. This is discussed further in section 4.3. In light of the general agreement between Gunn and Gott's condition and simulations of ram pressure stripping, it is assumed that a model based on this condition can be used to make general statements about where and to what extent galaxies are stripped.

The model for the group or cluster has two components, a gravitational potential in which the satellite orbits and an ICM against which the satellite shocks. The gravitational potential is modeled using an NFW profile with mass  $M_{v,gr}$ , radius,  $r_{v,gr}$ , and concentration,  $c_g$ . The scaled radius  $s \equiv r/r_{v,gr}$ .

$$\phi_{halo} = \frac{-GM_{v,gr}}{r_{v,gr}} g(c_g) \frac{\ln(1 + c_g s)}{s} \quad (2)$$

The NFW profile is discussed in more detail in appendix A. The ICM is modeled using a  $\beta$  profile with scale length  $r_c$ , and central density,  $\rho_0$ .

$$\rho = \rho_0 \left( 1 + \frac{r^2}{r_c^2} \right)^{(-3/2)\beta} \quad (3)$$

The  $\beta$  profile can be rewritten as

$$\rho = \frac{\alpha v_\rho \rho_c^0}{3} \left( 1 + \frac{s^2}{(r_c/r_{v,gr})^2} \right)^{(-3/2)\beta} \quad (4)$$

The parameter  $\alpha$  relates  $\rho_0$  to the characteristic density of the NFW profile, and  $v_\rho \rho_c^0$  is the average dark matter density within  $r_{v,gr}$ .

The gravitational potential of the satellite and the surface density of the gas disk are needed to model the restoring pressure. The gravitational potential combines a dark matter halo, a stellar disk, and a stellar bulge. The dark matter halo is modeled as an NFW profile

with mass  $M_{v,sat}$  and concentration  $c_s$ . The disk, of mass  $M_d$ , is described using a Miyamoto and Nagai potential (Miyamoto & Nagai 1975).

$$\phi_{disk} = \frac{-GM_d}{\sqrt{R^2 + (R_d + \sqrt{z^2 + h^2})^2}} \quad (5)$$

This potential is easily differentiated, and with the appropriate choice of disk scale length,  $R_d$ , and height,  $h$ , many of the properties of the potential of an exponential disk can be matched (Johnston et al. 1995). This potential can be rewritten as

$$\phi_{disk} = \frac{-GM_d}{R_d} \frac{1}{\sqrt{\lambda_d^2 S^2 + (1 + \sqrt{\lambda_d^2 z_s^2 + \lambda_h^2})^2}} \quad (6)$$

where  $\lambda_d \equiv r_{v,sat}/R_d$ ,  $\lambda_h \equiv h/R_d$ ,  $S \equiv R/r_{v,sat}$ , and  $z_s \equiv z/r_{v,sat}$ .

The bulge, of mass  $M_b$ , is described using a Hernquist potential (Hernquist 1990).

$$\phi_{bulge} = \frac{-GM_b}{r + r_b} \quad (7)$$

This can be written as

$$\phi_{bulge} = \frac{-GM_b}{r_b} \frac{1}{\lambda_b s_{sat} + 1} \quad (8)$$

where  $\lambda_b \equiv r_{v,sat}/r_b$ ,  $s_{sat} \equiv r_{sat}/r_v$ , and  $r_{sat}$  is the distance from the center of the satellite. By introducing  $m_{ds} \equiv M_d/M_{v,sat}$  and  $m_b \equiv M_b/M_{v,sat}$ , the full gravitational potential of the satellite can be written in the form

$$\phi_{full} = \frac{-GM_{v,sat}}{r_{v,sat}} f(s_{sat}, m_i, \lambda_i, c_s) \quad (9)$$

Gas in galaxies can be found in three spatial components: an exponential molecular gas disk with a scale length comparable to the stellar disk, a nearly flat atomic disk that extends beyond the stellar disk and shows a sharp cutoff, and a hot galactic halo. Beyond the disk cutoff, the atomic disk may continue as an ionized gas disk (Binney & Merrifield 1998).

The H I is modeled as a thin flat disk with mass  $M_g$ , surface density,  $\sigma_g$ , and a sharp cutoff at radius  $R_g$

$$\sigma_g = \begin{cases} \sigma_0, & R < R_g \\ 0, & R > R_g \end{cases} \quad (10)$$

$$\sigma_0 \equiv \frac{M_g}{\pi R_g^2} = \frac{M_{v,sat}}{r_{v,sat}^2} \frac{m_{dg} \lambda_g^2}{\pi} \quad (11)$$

where  $m_{dg} \equiv M_g/M_{v,sat}$  is the fractional mass of the gas and  $\lambda_g \equiv r_{v,sat}/R_g$  is the scaled size of the disk.

The inner gas disk is dominated by the  $H_2$  disk. The molecular disk is significantly more difficult to strip than the H I disk both because the  $H_2$  disk is more compact and because the  $H_2$  is found in molecular clouds. These clouds do not feel the effect of stripping as strongly as the diffuse H I. How stripping of  $H_2$  occurs and how the  $H_2$  clouds and diffuse H I in the inner disk interact are not known. The two phases may be tied together by magnetic fields; in which case the inner H I disk will remain until the ram pressure can remove the entire inner disk. It may also be possible for the wind to remove the

H I from the inner disk while leaving the  $H_2$  behind. Because of this uncertainty, the stripping of the inner disk will not be studied here. The model is only used to discuss stripping beyond 1.5 stellar scale lengths. If the ram pressure is not strong enough to affect the  $H_2$ , the  $H_2$  will contribute to the restoring pressure in the outer disk. Therefore, the mass of the  $H_2$  disk is added to the stellar mass.

The emphasis of this project is to study the stripping of the H I disk. However, the fate of the hot galactic halo can also influence the evolution of the stripped galaxy. It is expected that the hot halo will be easily stripped both because it is diffuse and because the restoring potential of the satellite is strongest in the disk. To check this a hot halo is included in the model galaxy.

Mori & Burkert (2000) give an analytic condition for the complete stripping of a hot galactic halo.

$$\rho_{ICM} v_{sat}^2 > P_{0,th} = \frac{\rho_{0,sat} k_B T}{\mu m_p} \quad (12)$$

where  $P_{0,th}$  and  $\rho_{0,sat}$  are the central thermal pressure and density of the hot galactic halo,  $k_B$  is the Boltzmann constant,  $T$  is the temperature of the galactic halo, and  $\mu m_p$  is the average molecular mass. The thermal pressure replaces the gravitational restoring pressure in the original stripping condition. In their simulations, this condition does a fair job of predicting the mass of a galaxy that can be completely stripped. This condition is adapted for the current model and all gas outside the radius where  $P_{ram} = P_{th}$  is assumed to be stripped.

The hot galactic halo is modeled by assuming that the gas is at the virial temperature,  $T_v$ , of the satellite and is in hydrostatic equilibrium in the satellite's dark matter potential. The self-gravity of the gas is ignored. The density of the hot halo is

$$\rho(s_{sat}) = \left( \frac{v_{\rho} \rho_0^c}{3} \right) m_{sg} j(s_{sat}, c_s) \quad (13)$$

where scaled density profile  $j(s_{sat}, c_s)$  is defined in appendix C and  $m_{sg}$  is the ratio of the mass of gas in the hot galactic halo to  $M_{v,sat}$ .

A dimensionless temperature,  $t(c_s)$  is also introduced in appendix C. It is defined by

$$t(c_s) \equiv \left( \frac{k_B T_v}{\mu m_p} \right) \left( \frac{r_{v,sat}}{GM_{v,sat}} \right) \quad (14)$$

It is a function of only  $c_s$ .

### 3. RESULTS

In this section the dependence of stripping on the masses of the large and satellite halos and on the model's parameters is explicitly determined.

The maximum ram pressure, the ram pressure at the pericenter of the galaxy's orbit, is given by

$$P_{ram,max} = \frac{GM_{v,gr}}{r_{v,gr}} \frac{b_s^2}{s_0^2} \frac{\epsilon}{\epsilon_v} \frac{\alpha v_p \rho_c^0}{3} \left( 1 + \frac{s_0^2}{(r_c/r_{v,gr})^2} \right)^{(-3/2)\beta} \quad (15)$$

where  $s_0$  is the distance of closest approach,  $\epsilon$  is the orbital energy per unit mass,  $\epsilon_v \equiv -GM_{v,gr}/r_{v,gr}$ ,  $b_s \equiv l^2/(\epsilon r_{v,gr}^2)$ , and  $l$  is the orbital angular momentum per unit mass. Both  $b_s$  and  $\epsilon/\epsilon_v$  are expected to be independent of the masses of the satellite and the cluster.

At any point in the orbit,  $s_{orbit}$ , the ram pressure is

$$P_{ram}(s_{orbit}) = \frac{2GM_{v,gr}}{r_{v,gr}} \frac{\alpha v_p \rho_c^0}{3} p(s_{orbit}, c_g) \quad (16)$$

where dimensionless pressure,  $p(s, c_g)$ , is defined.

$$p(s, c_g) \equiv \left[ g(c_g) \frac{\ln(1 + c_g s)}{s} - \frac{\epsilon}{\epsilon_v} \right] \left( 1 + \frac{s^2}{(r_c/r_{v,gr})^2} \right)^{(-3/2)\beta} \quad (17)$$

Equations for the orbital speeds are derived in appendix B. Assuming that  $\alpha$ ,  $\beta$ ,  $r_c/r_{v,gr}$ , and  $c_g$  do not depend on the mass of the halo, the  $M_{v,gr}$  dependence of both  $P_{ram}(s_0)$  and  $P_{ram}(s_{orbit})$  is  $P_{ram} \propto M_{v,gr}^{2/3}$ .

For a potential of the form in eq. 9, the force per unit gas mass in the  $z$  direction is found as follows.

$$f_z = \frac{GM_{v,sat}}{r_{v,sat}} \frac{\partial}{\partial z} f(s_{sat}, m_i, \lambda_i, c_s) \quad (18)$$

$$f_z = \frac{GM_{v,sat}}{r_{v,sat}^2} \frac{\partial}{\partial z} f(s_{sat}, m_i, \lambda_i, c_s) \quad (19)$$

Assuming that the  $m_i$  and  $\lambda_i$  introduced in section 2 and  $c_s$  are constant with mass, the mass dependence of the restoring force per unit gas mass is given by  $f_z \propto M_{v,sat}^{1/3}$ .

For the gas disk, if the fractional mass of the gas,  $m_{dg}$ , and the scaled size of the disk,  $\lambda_g$ , are both constant, then

$$\sigma_g \propto M_{v,sat}/r_{v,sat}^2 \propto M_{v,sat}^{1/3} \quad (20)$$

Combining the above,

$$P_{rest,max} = \sigma_g f_{z,max} \propto M_{v,sat}^{2/3} \quad (21)$$

For any radius along the disk,  $R_{str}$ , there is a maximum restoring pressure. If the maximum restoring pressure is greater than the ram pressure, the satellite holds the gas at this radius. The condition for the satellite holding its gas can be written as

$$\frac{P_{rest,max}}{P_{ram,max}} = \frac{M_{v,sat}^{2/3}}{M_{v,gr}^{2/3}} \frac{\left( \frac{\partial}{\partial z_s} \right)_{R_{str}} f(s_{sat}, m_i, \lambda_i, c_s) 2m_{dg} \lambda_g^2}{\alpha p(s_{orbit}, c_g)} > 1 \quad (22)$$

$$\frac{M_{v,sat}}{M_{v,gr}} > \left[ \frac{\alpha p(s_{orbit}, c_g)}{\left( \frac{\partial}{\partial z_s} \right)_{R_{str}} f(s_{sat}, m_i, \lambda_i, c_s) 2m_{dg} \lambda_g^2} \right]^{3/2} \quad (23)$$

The restoring pressure of the galactic hot halo is

$$P_{rest} = \left( \frac{GM_{v,sat}}{r_{v,sat}} \right) \left( \frac{v_p \rho_0^c}{3} \right) t(c_s) m_{sg} j(s_{sat}, c_s) \quad (24)$$

The condition for retaining this gas within  $s_{sat}$  is

$$\frac{M_{v,sat}}{M_{v,gr}} > \left[ \frac{t(c_s) m_{sg} j(s_{sat}, c_s)}{2\alpha p(s_{orbit}, c_g)} \right]^{3/2} \quad (25)$$

If the model's parameters:  $c_g$ ,  $c_s$ ,  $\epsilon/\epsilon_v$ ,  $b_s$ ,  $\beta$ ,  $r_c/r_{v,gr}$ ,  $\alpha$ , the  $m_i$ , and the  $\lambda_i$ ; are all independent of the mass of the satellite and cluster, then the fraction of gas that is stripped from a satellite depends on the ratio  $M_{v,sat}/M_{v,gr}$ . In this case,  $P_{ram} \propto M_{v,gr}^{3/2}$  and for both the gas disk and hot galactic halo  $P_{rest} \propto M_{v,sat}^{3/2}$ .

Assuming that this set of parameters is constant is equivalent to assuming that the physical parameters scale with mass in the most obvious way. It assumes that component masses scale as  $M_v$ , lengths scale as  $r_v$ , and the central densities of the ICM and the satellite's hot galactic halo are constant. For any model in which these scalings hold, the result that the extent of stripping depends on  $M_{v,sat}/M_{v,gr}$  will hold. For any cluster mass, the scaled radius will set the ICM density and the orbital velocity will be proportional to  $M_{v,gr}/r_{v,gr}$ . The restoring pressure depends on the depth of the satellite galaxy's gravitational potential well and the density of the gas disk. For a generic potential,  $\phi \propto M_{v,sat}/r_{v,sat}$  and the restoring force per unit gas mass is proportional to  $M_{v,sat}^{1/3}$ . If the mass of the gas disk scales with  $M_{v,sat}$  and the disk length with  $r_{v,sat}$ , then the density of the gas disk scales as  $M_{v,sat}^{1/3}$  and the restoring pressure as  $M_{v,sat}^{2/3}$ .

#### 4. MODEL PARAMETERS

In this section a reference set of values for the model's parameters is introduced and the effect of varying these parameters is discussed. The reference parameters determine the values of  $M_{v,sat}/M_{v,gr}$  at which stripping occurs. They are taken from observations, where possible, and  $\Lambda$ CDM simulations, otherwise. Two types of parameter variations are discussed. First, several of the model parameters vary systematically with  $M_{v,sat}$  or  $M_{v,gr}$ . Second, at fixed masses the parameters have scatter.

The scatter in the parameters is discussed for several reasons. By combining an estimate for the scatter in each parameter with the model, the parameters that have the most effect on the radius to which an individual galaxy is stripped can be identified. Second, it is useful to know the range of ratios across which stripping occurs. Finally, if the overall scatter is not too large, the relationship between  $R_{str}$  and  $M_{v,sat}/M_{v,gr}$  could be used to search for signs of stripping in a large galaxy survey. The results of this section are discussed in the terms above in section 5.2.

In Figures 1 and 2, the  $M_{v,sat}$  at which a satellite is stripped is plotted versus  $R_{str}/R_g$  and  $M_{str}/M_g$  for a satellite orbiting at a variety of  $s_{orbit}$  values in  $10^{15}$ ,  $10^{14}$ , and  $10^{13} M_\odot$  clusters. The mass of the stripped gas is denoted as  $M_{str}$ . Table 1 lists the model parameters used for three models, a large satellite in a  $10^{15} M_\odot$  cluster, the reference model; a large satellite in a  $10^{14} M_\odot$  cluster, the middle-mass model; and a small satellite in a  $10^{13} M_\odot$  group, the low-mass model. The large satellite model is based on the Milky Way. Physical length scales and masses for the stellar disk and bulge are from Johnston et al. (1995). The stellar disk is modeled using  $M_{ds} = 10^{11} M_\odot$ ,  $R_d = 6.4$  kpc, and  $h = .26$  kpc. The equivalent  $R_d$  for an exponential disk is 5 kpc. The bulge is modeled using  $M_b = 3.4 \times 10^{10} M_\odot$  and  $r_b = .7$  kpc. A flat disk with a radius of 30 kpc gives  $R_g/R_d$  similar to that seen in observations. The H I gas mass is chosen to result in a disk density of  $5 M_\odot pc^{-2}$ . The virial mass is chosen such that  $M_{v,sat}/M_{baryon} \approx 12$ . Setting  $M_{v,sat}$  also sets  $r_{v,sat}$ . The concentrations used are  $c_s = 12$  and  $c_g = 5.5, 7.5$ , and  $10$ . The concentrations are based on Bullock et al. (2001) and assume an

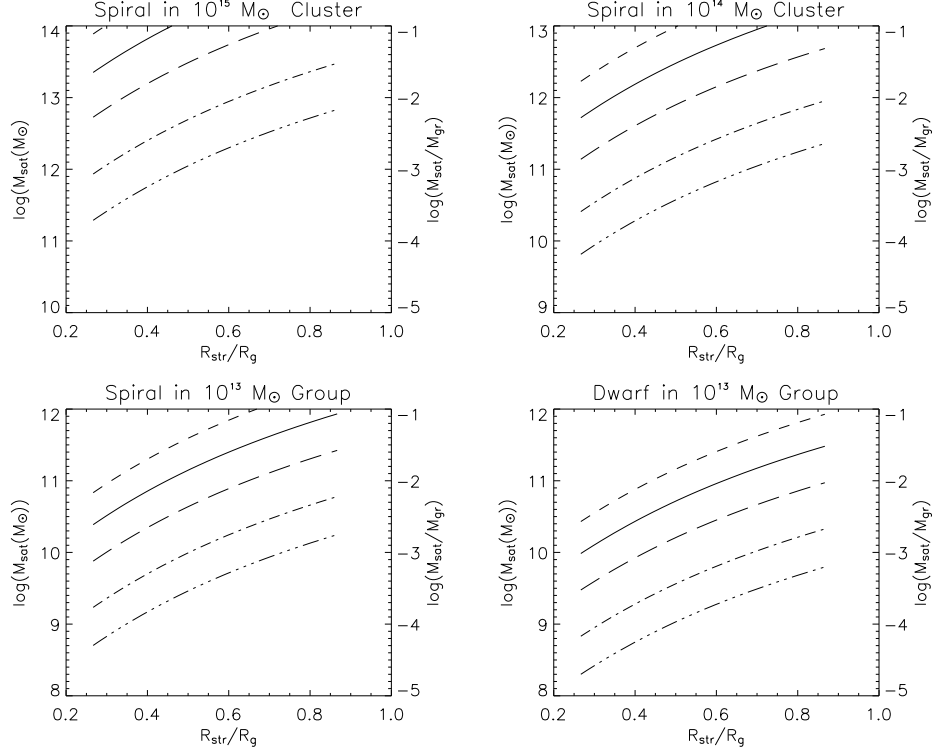


FIG. 1.— Mass at which a satellite's gas disk is ram pressure stripped versus  $R_{\text{str}}/R_d$ . Short-dashed line:  $s_{\text{orbit}} = .25$ , solid:  $s_{\text{orbit}} = .35$ , long-dash:  $s_{\text{orbit}} = .5$ , dash-dot:  $s_{\text{orbit}} = .75$ , dash-triple-dot:  $s_{\text{orbit}} = 1$ . Top-left: Spiral galaxy orbiting in a  $10^{15} M_{\odot}$  cluster. Top-right: Spiral galaxy orbiting in a  $10^{14} M_{\odot}$  cluster. Bottom-left: Spiral galaxy orbiting in a  $10^{13} M_{\odot}$  group. Bottom-right: Dwarf galaxy orbiting in a  $10^{13} M_{\odot}$  group.

average over-density within  $r_v$ ,  $v_{\rho}$ , of 337. The assumed over-density affects the concentrations, which are measured using  $v_{\rho} = 337$ , and  $\alpha$ , because it relates the ICM and dark matter densities. Note that  $v_{\rho}$  does not appear in equation 23 or 25. The ICM parameters,  $\alpha$ ,  $\beta$ , and  $r_{v,gr}/r_c$ , are set by X-ray observations of clusters and groups, and the orbital parameters are taken from simulations. Both are discussed below. Table 1 also lists the assumed scatter in each model parameter and resulting scatter in the mass at which a satellite is stripped.

#### 4.1. ICM Profile

The profile of the ICM is determined by the parameters  $\alpha$ ,  $r_{v,gr}/r_c$ , and  $\beta$  (eq. 4). Sanderson & Ponman (2003) compile a set of average ICM profiles for clusters with temperatures ranging from 0.3 to 17 keV. They find that the ICM of groups and poor clusters is both less dense and more extended than in rich clusters. Mohr et al. (1999) present X-ray observations of a set of clusters and Helsdon & Ponman (2000) and Osmond & Ponman (2004) present X-ray observations of groups. The three groups present  $\beta$  and  $r_c$  (in units of kpc) for a best-fit  $\beta$  profile and the X-ray temperature,  $T_X$ , for each group or cluster. The average  $\beta$  and  $r_{v,gr}/r_c$  for the cluster observations are approximately 0.67 and 12. The averages for the group observations are approximately 0.45 and 170. To convert  $r_c$  (in kpc) to  $r_c/r_{v,gr}$ , virial masses for the groups and clusters are found using the  $M_{200}(T_X)$  relationship from Popesso et al. (2005). The mass  $M_{200}$  is the mass contained within the radius at which the average over-density reaches 200. It is con-

verted to  $M_v$  using equations A7 and A6. The profiles in Sanderson & Ponman (2003) are scaled using  $r_{200}$  as determined in Sanderson et al. (2003). The differences in the  $r_c/r_{v,gr}$  determined using the two  $M_{200}(T_X)$  relationships are within the intergroup scatter in  $r_c/r_{v,gr}$ . The average profiles for the hottest and coolest groups from Sanderson & Ponman (2003) are well matched by using  $\alpha = 6.5$  and 20 respectively and the appropriate  $\beta$  and  $r_{v,gr}/r_c$ . In Figures 1 and 2, plots are made for stripping in  $10^{13}$ ,  $10^{14}$ , and  $10^{15} M_{\odot}$  clusters. A cluster with  $M_{v,gr} = 10^{15} M_{\odot}$  falls into the hottest temperature bin from Sanderson & Ponman (2003) while a group with  $M_{v,gr} = 10^{13} M_{\odot}$  falls into the coolest. The ICM parameters for the  $10^{14} M_{\odot}$  cluster are  $\alpha = 5.5$ ,  $\beta = .57$ , and  $r_{v,gr}/r_c = 25$ .

Scatter in these parameters is estimated using the three sets of observations. The observed scatter in  $\beta$  is  $\pm 0.08$ . The majority of clusters have  $r_{v,gr}/r_c$  between 7 and 20, and groups have  $r_{v,gr}/r_c$  between 75 and 270. For both groups and clusters,  $\alpha$  is assumed to vary by a factor of  $\sqrt{6}$  in either direction. Varying  $\beta$  varies the ram pressure at  $s_{\text{orbit}} = .35$  by a factor of 2 for the clusters and a factor of 7.4 for the groups. The ram pressure varies by a factor of 6 in the clusters and 5.4 in the groups when  $r_{v,gr}/r_c$  is varied. Varying  $\alpha$  by a factor of 6 results in an increase in the ram pressure by the same factor.

#### 4.2. Orbits

The orbital parameters are important for determining both satellites' pericenters and orbital speeds. In theory, the pericenter of a satellite's orbit is determined by  $\epsilon/\epsilon_v$

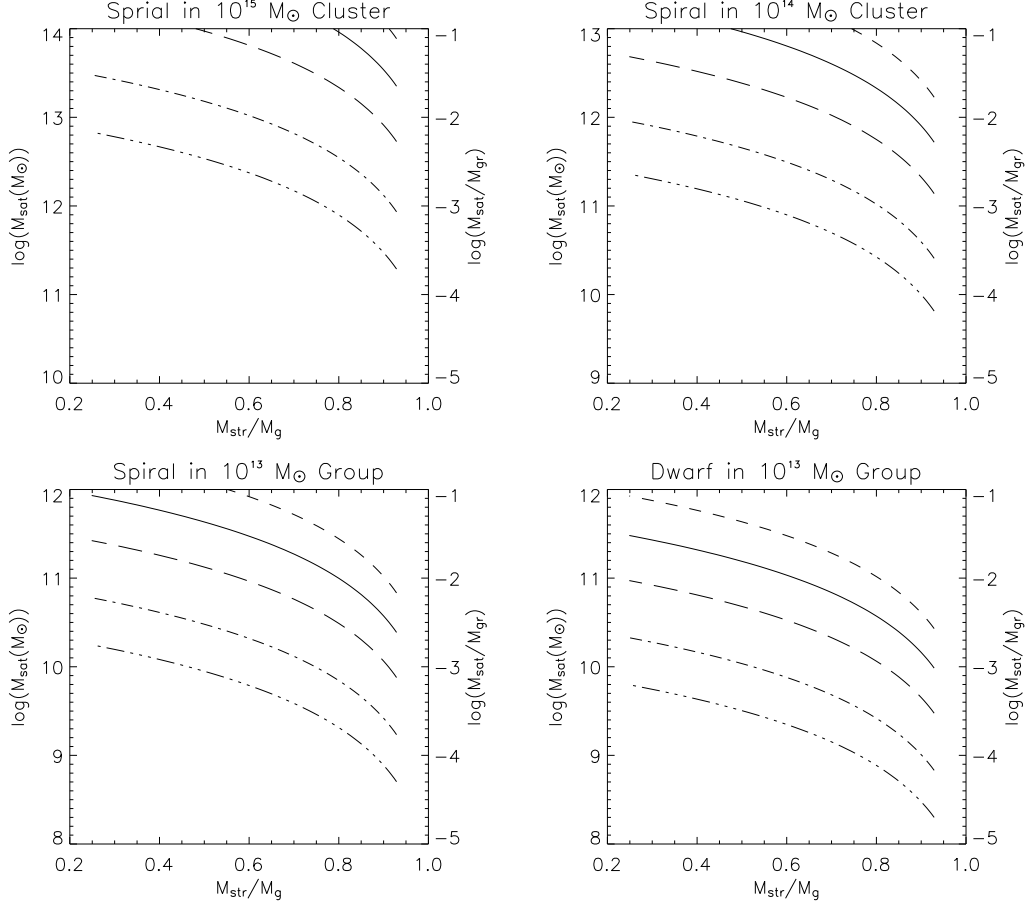


FIG. 2.— Mass at which a satellite's disk is ram pressure stripped versus the mass fraction of gas disk that is stripped. Lines are the same as in Fig. 1. *Top-left*: Spiral galaxy orbiting in a  $10^{15} M_{\odot}$  cluster. *Top right*: Spiral galaxy orbiting in a  $10^{14} M_{\odot}$  cluster. *Bottom left*: Spiral galaxy orbiting in a  $10^{13} M_{\odot}$  group. *Bottom right*: Dwarf galaxy orbiting in a  $10^{13} M_{\odot}$  group.

and  $b_s$  (Eq. B2). However, Gill et al. (2004) present pericenter distributions for subhalos at  $z = 0$  in cluster-sized dark matter halos with  $M_{v,gr} = 1 - 3 \times 10^{14} M_{\odot}$ . They find that the  $s_0$  distribution can be fit with a Gaussian with  $\bar{s}_0 = .35$  and  $\sigma_{s_0} = .12$ . This distribution shows little variation with either  $M_{v,gr}$  or  $M_{v,sat}$ . The maximum ram pressure in a cluster with ICM parameters corresponding to a few  $10^{14} M_{\odot}$  and  $c_g = 7.5$  increases by a factor of 5.4 when the pericenter decreases from  $s_0 = 0.47$  to 0.23.

Some satellites have not yet passed through the pericenter of their orbits, and the maximum ram pressure they have experienced is determined by their current  $s_{orbit}$ . Increasing  $s_{orbit}$  from 0.35 to 1 results in a decrease of the mass at which a satellite can be stripped by two orders of magnitude. Therefore, unless it is known that a group of satellites have all passed through their pericenters, the effect of varying  $s_{orbit}$  cannot be treated like the scatter in the other parameters. Instead, when comparing satellites in different environments or with different masses,  $s_{orbit}$  must be specified.

At a given  $s_{orbit}$ , the ram pressure is dependent on  $\epsilon/\epsilon_v$ , but not  $l/l_v$ . In simulations Vitvitska et al. (2002) find that the speeds of satellites entering dark halos can be fit with a Maxwell-Boltzmann distribution with  $v_{rms}^2 \approx 1.15 v_c^2$ ,  $v_c^2 \equiv GM_{v,gr}/r_{v,gr}$ . The total energy per unit mass of an object at the virial radius with

this speed is  $\epsilon \approx \epsilon_v$ , and is a weak function of  $c_g$ . This distribution has a large scatter,  $\sigma_v = .6v_c$ , corresponding to  $\epsilon/\epsilon_v$  between 0.2 and 2.8. At  $s_{orbit} = .35$ , when  $v_{sat}(s_{orbit} = 1)/v_c$  is varied between 0.55 and 1.75, the  $M_{v,sat}/M_{v,gr}$  needed for stripping vary by a factor of  $\approx 1.6$ . Vitvitska et al. (2002) also find that for  $M_{v,sat} < .4M_{v,gr}$  the angular momenta of satellites entering halos can be fit with a Maxwell-Boltzmann distribution with  $l_{rms}/l_v = .7$ ,  $l_v \equiv v_c r_v$ . As expected, the distributions of  $\epsilon/\epsilon_v$  and  $b_s$  do not depend on  $M_{v,sat}$  and  $M_{v,gr}$ . However, unless the correlation between  $v_{sat}(s_{orbit} = 1)/v_c$  and  $l/l_v$  is understood, these parameters cannot be used to determine the distribution of  $s_0$ .

### 4.3. Inclination

The Gunn and Gott condition assumes that all galaxies orbit in a face-on wind. In reality, galaxies orbit at all inclinations. Simulations show that galaxies are stripping at all inclinations, but edge-on galaxies are stripped to larger radii than face-on galaxies.

Marcolini et al. (2003) point out that while galaxies that are hit face-on by the ICM wind experience the most ram pressure stripping, galaxies in an edge-on wind experience the most viscous stripping. They derive an expression for the ram pressure needed to viscously strip an edge-on galaxy to radius  $R$  and treat this pressure as a restoring pressure for the edge-on case. When they

compared the new condition to the Gunn and Gott condition, they find that any ram pressure that can completely strip a face-on galaxy will viscously strip an edge-on galaxy and that any ram pressure that cannot strip a face-on galaxy will not strip an edge-on galaxy. The two models differ when a galaxy is partially stripped. In this case edge-on galaxies are still stripped, but to larger radii than face-on galaxies. They run simulations at a variety of inclination angles,  $i$ , and find that the final stripping radii match the predictions of the two conditions. When galaxies at intermediate angles are partially stripped, they are stripped to intermediate radii.

When Marcolini et al. plot the two restoring pressures for three galaxy masses, 0.76, 7.4, and  $77.2 \times 10^9 M_\odot$ , their Figure 3, the fractional difference between the two restoring pressures is close to constant throughout the outer disk but increases with the mass of the galaxy. For the largest galaxy the restoring force in the edge-on case is  $\approx 4.5$  times larger.

#### 4.4. Concentration of the Cluster

Small dark matter halos tend to be more concentrated than large dark matter halos. Bullock et al. (2001) use an analytical model of the evolution of dark matter halos to describe this dependency. For the standard  $\Lambda$ CDM model, near  $M_v = M_* \approx 1.5 \times 10^{13} h^{-1} M_\odot$  they find

$$c(z=0) = 9 \left( \frac{M_v}{M_*} \right)^{-0.13} \quad (26)$$

The  $c_g$  used for the cluster and group models are determined using this relation. Bullock et al. (2001) also see a scatter that is as large as the evolution of the concentration over the range  $0.01 M_* < M_v < 100 M_*$ . To explore the scatter introduced through  $c_g$ ,  $c_g$  is varied between 5 and 16.

The cluster concentration affects both  $s_0$  and the ram pressure at a given  $s_{\text{orbit}}$  (eqs. B2 and B6). When  $c_g$  is increased from 5 to 16, for  $v_{\text{sat}}^2(s_{\text{orbit}} = 1) = 1.15 v_c^2$  and  $l/l_v = 0.7$ , the pericenter decreases from  $s_0 = 0.53$  to 0.5. This is smaller than the scatter in the pericenter. At a given  $s_{\text{orbit}}$ , the orbital speed increases slightly as  $c_g$  increases. This difference increases as  $s_{\text{orbit}}$  decreases. For  $s_{\text{orbit}} = 0.75$ , the change is not noticeable. For  $s_{\text{orbit}} = 0.35$ , the  $M_{v,\text{sat}}/M_{v,\text{gr}}$  at which a satellite is stripped increases by a factor of 1.2 when  $c_g$  is increased from 5 to 16.

#### 4.5. Concentration of the Satellite

In the outer H I disk the restoring pressure of the dark matter halo makes a non-negligible contribution to the restoring pressure. More concentrated satellites have higher restoring pressures than other satellites of the same mass. Varying  $c_s$  between 12 and 20 varies the  $M_{v,\text{sat}}/M_{v,\text{gr}}$  at which stripping occurs by a factor of  $\approx 1.7$ .

The concentration also alters how the hot galactic halo is stripped. In a more concentrated dark matter halo the gas is denser in the center and more diffuse elsewhere. Stripping can therefore occur down to a smaller radius, but a smaller fraction of the gas is lost.

#### 4.6. Length Ratios, $\lambda_i$

How disk scale lengths vary with  $M_{v,\text{sat}}$  is an open question. Theory suggests that when cold gas disks form in dark matter halos, their initial radii are proportional to the virial radii of the halos they form in (Mo et al. 1998). There is a large scatter in this relationship that is due to a large scatter in the disk angular momenta. However, cold disks are composed of a combination of stars and gas, and how these components arise from the original cold disk is not understood.

The fraction of the H I that is found in the outer disk, where the restoring force from the stellar disk is weakest, is set by the ratio  $\lambda_d/\lambda_g$  (eqs. 6 and 11). Swaters et al. (2002) observed the H I disks of 73 local dwarfs. They found  $\lambda_d/\lambda_g = 6 \pm 2.5$  for the dwarfs. For late-type spirals  $\lambda_d/\lambda_g = 5.5 \pm 1.6$ . These observations suggest that  $\lambda_d/\lambda_g$  contributes to the scatter in  $M_{v,\text{sat}}/M_{v,\text{gr}}$ , but not to the mass dependence. Varying  $\lambda_d/\lambda_g$  changes both the size and the shape of the restoring force. When  $\lambda_g$  is held at 5.7 and  $\lambda_d/\lambda_g$  is decreased to 3.5, the restoring force decreases within  $R/R_g = 0.45$  and increases at larger  $R$ . The fractional change in  $P_{\text{rest}}$  is less than 1.1 throughout the disk. Holding  $\lambda_g$  constant and increasing  $\lambda_d/\lambda_g$  to 8.5, results in decreasing the restoring force outside of  $R/R_g = 0.3$  by a factor of less than 1.13.

Varying  $\lambda_g$  while holding  $\lambda_d/\lambda_g$  constant changes the density of both the gas and stellar disks. At a given  $R/R_g$ , the density of both disks  $\propto \lambda_g^2$  and the restoring pressure  $\propto \lambda_g^4$ . The scatter in  $\lambda_g$  and how  $\lambda_g$  evolves with mass are not known. However, because of the heavy dependence of the restoring pressure on it, the scatter in  $\lambda_g$  is likely to make an important contribution to the scatter in the  $M_{v,\text{sat}}/M_{v,\text{gr}}$  at which stripping occurs. Increasing  $\lambda_g$  from  $0.75 \lambda_g$  to  $1.25 \lambda_g$  decreases the  $M_{v,\text{sat}}/M_{v,\text{gr}}$  needed for stripping by a factor of 20.

The presence of molecular gas complicates the physics of stripping in the inner disk. Therefore, this model is only applied to disk radii beyond 1.5 stellar disk scale lengths. At these radii,  $R > 10r_b$ , the bulge acts as a point mass, and changing  $\lambda_b$  (Eq. 8) has no effect. In particular, the radius of the bulge changes with the mass of the bulge. Below, the mass of the bulge is allowed to vary by 40%. Assuming that  $r_b \propto M_b^{1/3}$ , this corresponds to allowing  $r_b$  to vary by 12%. This is not noticeable in the outer H I disk.

#### 4.7. Mass Fractions, $m_i$

Both  $m_b$  and  $m_{dg}$  (eqs. 8 and 11) are correlated with the mass of the satellite. While the majority of large spiral galaxies have a significant fraction of their stars in a stellar bulge, low-mass late-type galaxies do not. Very low mass spiral galaxies exist that do not contain any bulge (Matthews & Gallagher 1997) and dwarf galaxies are observed to be either dE/dSph or dIrr. In addition, low-mass late-type galaxies have a higher fraction of their mass in the gas disk than large spirals (Swaters et al. 2002). Decreasing  $m_b$  reduces the restoring pressure in the outer disk. In contrast, increasing  $m_{dg}$  increases the restoring pressure.

In the bottom right panels of Figures 1 and 2, the satellite is bulgeless, the gas mass fraction,  $m_{dg}$ , is doubled, and the stellar mass fraction,  $m_{ds}$ , is reduced by 20%. The original model corresponds to a large late-type spiral, while the bulgeless model is closer to a late-

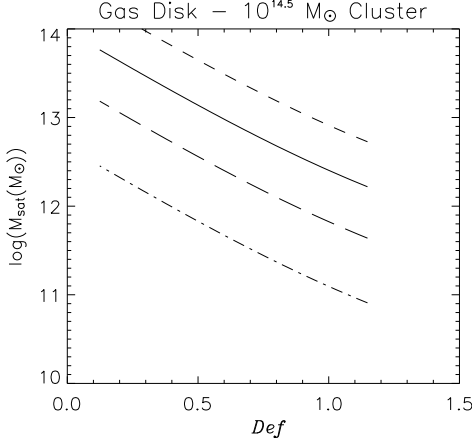


FIG. 3.— Mass at which a satellite's gas disk is ram pressure stripped versus the deficiency in a  $3.5 \times 10^{14} M_{\odot}$  cluster. Lines are the same as in Fig. 1.

type dwarf galaxy. Because the restoring force due to the bulge is small, the net effect is to increase the restoring pressure. Most galaxies will lie between the two plotted models.

The  $m_i$  can be split between those that set the depth of the potential well,  $m_{ds} + m_{H_2}$  and  $m_b$ , and  $m_{dg}$  which sets the gas density. In late-type galaxies, bulges can contribute up to 50% of the stellar light (Binney & Merrifield 1998). In the reference model, 25% of the stars are in the bulge. Varying  $m_b$  between 15% and 35% of the satellite's stars, varies the restoring force in the outer disk by a factor of  $\approx 1.1$ . Neither the mass dependence nor the scatter in  $m_{ds} + m_{H_2}$  are known. Varying  $m_{ds} + m_{H_2}$  by 20%, varies the restoring force by a factor of  $\approx 1.3$ . The effect of scatter in the gas density parameter,  $m_{dg}$ , is straight forward. The  $M_{v,sat}/M_{v,gr}$  at which stripping occurs varies as  $m_{dg}^{-3/2}$ . Varying  $m_{dg}$  by a factor of 1.5, similar to the scatter in  $M_{HI}/L_R$  in Figure 9 of Swaters et. al., varies the  $M_{v,sat}/M_{v,gr}$  needed for stripping by a factor of 1.8.

Variations in the  $m_i$  values should be correlated because the variation in the mass in baryons in a satellite is likely smaller than the variation in the mass of a given component. The correlation is such that it will reduce the overall scatter.

## 5. DISCUSSION

### 5.1. Comparison with Observations and Simulations

In this section, the  $M_{v,sat}/M_{v,gr}$  values at which the model predicts stripping should occur are compared to observations of H I disks from Solanes et al. (2001). This sample is useful for making comparisons between the model and observations because the number of spirals is large and the observations span several clusters. The average temperature of the clusters is 3.5 keV. This corresponds to  $M_{v,gr} = 3 \times 10^{14} M_{\odot}$ . The average gas profile for this temperature can be described using the middle mass cluster model. In Figure 4 from Solanes et al. the fraction of spirals with  $def > 0.3$  and the average deficiency are plotted versus  $r/R_A$ , where  $R_A$  is the Abel radius. In Figure 3 of the present paper  $M_{v,sat}$  is plotted versus the deficiency in a  $3 \times 10^{14} M_{\odot}$  cluster at several  $s_{orbit}$ . The deficiency is defined as

$def \equiv \log(\bar{M}/M_{obs})$ , where  $M_{obs}$  is the observed H I mass and  $\bar{M}$  is the average H I mass for field spirals with the same morphology and optical diameter. For the model  $def = \log(M_g/(M_g - M_{str}))$ .

The observed fraction of spirals with  $def > 0.3$  reaches 0.3 at  $r/R_A \approx 1$ , and 0.45 at  $r/R_A \approx 0.5$ . The model predicts that almost all galaxies within  $s_{orbit} = 0.5$  have  $def > 0.3$ . However, only  $\approx 30\%$  of the galaxies viewed within  $r/r_{v,gr} = 0.5$  actually reside within  $r/r_{v,gr} = 0.5$ . This estimate assumes that the galaxy distribution follows an NFW profile and that all galaxies within  $r/r_{v,gr} = 2$  are included in the projected cluster. At  $s_{orbit} = 1$ , the model predicts that an average galaxy traveling face-on to the wind is stripped to  $def > 0.3$  for  $M_{v,sat} < 10^{11.5} M_{\odot}$ . This estimate can be roughly adjusted for inclination by multiplying by  $10^{-5}$ ,  $M_{v,sat} < 10^{11} M_{\odot}$ . Approximately 45% of the galaxies seen within  $s_{orbit} = 1$  actually reside within  $s_{orbit} = 1$ . Some galaxies beyond the  $s_{orbit}$  under consideration will be stripped to  $def > 0.3$ . Therefore, the observed fraction of spirals with  $def > 0.3$  should be greater than that predicted by multiplying the volume fraction with the fraction of stripped galaxies within  $s_{orbit}$ . This condition is met for  $s_{orbit} = 1$  if at least a third of the observed spirals have  $M_{v,sat} > 10^{11} M_{\odot}$ , corresponding to  $M_d \approx 8 \times 10^9 M_{\odot}$ . For  $s_{orbit} = 0.5$ , the volume fraction is lower than the observed fraction and this condition is easily met. The difference between the observed value and product of the volume fraction and stripped fraction should decrease as  $s_{orbit}$  increases. A  $10^{11} M_{\odot}$  spiral traveling face-on to the wind is stripped to  $def \approx 1$  at  $s_{orbit} = 0.8$ . A  $10^{12} M_{\odot}$  spiral traveling face-on to the wind is stripped to  $def \approx 1$  at  $s_{orbit} = 0.4$ . Spirals with  $def \approx 1$  are not observed in the Solanes et al. (2001) sample outside of  $1R_A$ .

The model does a good job of matching the observations of H I disks from Solanes et al. (2001). If the model over-predicted the degree of stripping, then it would over-predict the fraction of spirals with  $def > 0.3$  and predict deficiencies at large radii greater than those observed. If the model under-predicted the degree of stripping, then it might not predict that spirals in the center of the cluster can have  $def \approx 1$  and would require that a larger fraction of the observed spirals reside in the cluster center.

Both Marcolini et al. (2003) and Roediger & Hensler (2005) run simulations of disk galaxies in winds typical of the outskirts of a group, equivalent to  $s_{orbit} = 1$  and 0.7, and the center of a group,  $s_{orbit} = 0.2$  and 0.25. In Marcolini et al. the two lowest mass simulated dwarfs are completely stripped in the high ram pressure. In the other cases, the dwarfs are partially stripped to a range of radii. When the gas surface density in the current model is adjusted to the exponential gas density in the dwarf models, the current model and the simulations match well for both  $s_{orbit}$ . The only disparity is that for  $s_{orbit} = 0.2$  the high-mass model is stripped to  $R_{str}/R_g = 0.1$  in the simulations and to  $R_{str}/R_g = 0.45$  in the model. This is probably due to differing dark matter halo profiles. The high-mass,  $M > 10^{11} M_{\odot}$ , galaxy model of Roediger and Hensler is stripped to  $R_{str}/R_g = 0.8$  in the lower ram pressure and  $R_{str}/R_g = 0.6$  in the higher ram pressure. After the gas

density is adjusted, the stripping radii of their high-mass model in the two winds are matched well by the model.

### 5.2. Model Predictions

In this model there exist three stripping regimes, stripping of the hot galactic halo, the flat H I disk, and the inner gas disk. The focus is on stripping of the flat H I disk. However, the model also includes a hot galactic halo. This hot gas is easily stripped in all environments. A satellite galaxy that is orbiting at  $s_{orbit} = 1$ , and has a hot galactic halo consisting of 0.5% of its mass, is stripped of at least 40% of its hot halo. At  $s_{orbit} = 0.35$ , a typical pericenter, all satellite galaxies are stripped of practically their entire halo in both groups and clusters. The stripping of the inner disk has not been studied. However, this gas should be difficult to strip and any spiral that has not been stripped of its entire outer H I disk should retain this gas. The rest of this section focuses on the outer disk.

The model does a reasonable job of matching H I observations in large cluster spirals. Therefore, it can be used to predict the extent of stripping at different  $M_{v,sat}$  and  $M_{v,gr}$ . The model's basic prediction, that the stripping radius is determined by the ratio  $M_{v,sat}/M_{v,gr}$  is modified by the mass dependence of the model's parameters. Therefore, the usefulness of the model's predictions depends in part on how well this dependence is understood. Fortunately, the mass dependence of many of the parameters is based on observations. The model parameters that most alter  $M_{str}(M_{v,sat}/M_{v,gr})$  in low-mass systems are the ICM profile parameters and the distribution of mass in the galaxy. The scaled ram pressure,  $P_{ram}/M_{v,gr}^{2/3}$ , that a satellite experiences decreases with  $M_{v,gr}$  because the ICM density throughout most of the cluster decreases. The scaled restoring pressure,  $P_{rest}/M_{v,sat}^{2/3}$ , is larger in low-mass disks because a higher fraction of the disk mass is found in the H I disk. The changes in both the scaled ram and restoring pressures act to decrease the  $M_{v,sat}/M_{v,gr}$  at which stripping occurs in low-mass systems. For example, the Local Group dwarfs have  $M_{v,sat}/M_{v,gr}$  smaller than the bright spirals in Virgo but should experience similar amounts of stripping.

The model makes three basic predictions. Dwarf galaxies are stripped of their entire outer H I disks in clusters and lose varying fractions of their outer disk in groups. Massive spirals can also be stripped of significant fractions of their H I disk in groups if they travel to small  $s_{orbit}$ . In a  $10^{13} M_{\odot}$  group, a  $10^{10} M_{\odot}$  dwarf is stripped of 50% of its H I disk at  $s_{orbit} = 0.7$ , a  $10^{11} M_{\odot}$  satellite is similarly stripped at either  $s_{orbit} = 0.5$  or  $s_{orbit} = 0.35$ , depending on the satellite model used, and a large  $5 \times 10^{11} M_{\odot}$  satellite is similarly stripped at  $s_{orbit} = 0.3$ . The corresponding orbits from stripping 80% of the H I disk are  $s_{orbit} = 0.55, 0.35, 0.25$ , and  $0.2$ . It should be kept in mind that these numbers are for an average satellite traveling face-on to the ICM wind.

The degree of stripping that a particular satellite of mass  $M_{v,sat}$  experiences orbiting in a cluster of mass  $M_{v,gr}$  can vary greatly. The parameters that are responsible for most of the variation in  $M_{str}$  are the ICM parameters,  $\alpha, \beta, r_{v,gr}/r_c$ , the galaxy's inclination,  $i$ , the pericenter,  $s_0$ , and the extent of the disk,  $\lambda_g$ . The varia-

tion in the stellar and gas surface densities is largely contained in  $\lambda_g$ . The ICM parameters are set by the choice of cluster, but clusters contain galaxies with a variety of orbits, morphologies, and inclinations. Within the same cluster, a galaxy of mass  $M_{v,sat} = M$  with a low surface density on a radial orbit traveling face-on to the wind can be as severely stripped as a galaxy with  $M_{v,sat} \approx M/25$  that has a high surface density and is traveling edge-on. At the same time, the ram pressure can vary significantly between clusters with the same mass because of variations in the ICM profile. Two identical satellite galaxies on identical orbits in different clusters of the same mass can experience ram pressures that vary by a factor of  $\approx 10$ .

An effective mass,  $M_{eff}$ , can be defined for each individual galaxy. This is the mass of a satellite that the model predicts is stripped to the same  $R_{str}$  as the given galaxy. The effect of the scatter in the parameters can then be discussed in terms of the scatter in  $M_{eff}$  at a given  $M_{v,sat}$ . The scatter in the  $M_{v,sat}/M_{v,gr}$  at which a galaxy is stripped of  $M_{str}$ , or in  $M_{eff}$ , can best be expressed as a multiplicative factor,  $\log(M_{eff}) = \log(M_{v,sat}/M_{v,gr}) \pm \sigma_{log}$ . The source of scatter in  $M_{eff}$  can be grouped into three types, that due to the ICM parameters,  $\alpha, \beta, r_{v,gr}/r_c$ , the orbital parameters,  $\epsilon/\epsilon_v, i, c_g$ , and the restoring pressure parameters,  $c_s, m_i, \lambda_i$ . The overall scatter in the high- and low-mass models, the result of varying all of the model parameters, are  $\sigma_{log,h} \approx 0.75$  and  $\sigma_{log,l} \approx 0.85$ . These can be broken down into  $\sigma_{log,ICM,h} = 0.7, \sigma_{log,ICM,l} = 0.8, \sigma_{log,orbit} = 0.5$ , and  $\sigma_{log,rest} = 0.65$ . The discussion in the paragraph above is based on these estimates.

The uses of this model are twofold. First, it makes general predictions about the degree of stripping that occurs to galaxies of different masses in a range of environments. Second, it links the degree of stripping,  $M_{str}$  or  $R_{str}$ , to the ratio  $M_{v,sat}/M_{v,gr}$ . This may be useful for verifying whether stripping is occurring within a galaxy catalog. The size of the scatter in  $M_{eff}$  determines the size of the galaxy catalog that is needed to see a dependence of  $M_{str}$  on  $M_{v,sat}/M_{v,gr}$ . The scatter in the  $\beta$  profile parameters is a major contributor to the scatter in  $M_{eff}$ . Therefore, such a catalog must either contain many clusters, or the ICM profile of the clusters must be known. As an estimate of the catalog size necessary, if 200 satellite galaxies with approximately the same  $M_{v,sat}$  orbiting in 50 groups or clusters with the same  $M_{v,gr}$  are combined, then  $\log(\bar{M}_{eff}) \approx \log(M_{v,sat}) \pm .25$ . If the range in  $M_{v,sat}$  and  $M_{v,gr}$  of such a catalog is large compared to this scatter, then the effects of stripping should be seen in the relationship between  $M_{str}$  and  $M_{v,sat}/M_{v,gr}$ .

## 6. CONCLUSIONS

The model developed here relates the degree of ram pressure stripping a satellite galaxy experiences to the galaxy and cluster masses and can be used to quickly determine the extent to which a galaxy is likely to be stripped. All galaxies lose most of their hot galactic halo. In clusters galaxies at moderate mass ratios,  $M_{v,sat}/M_{v,gr} \approx 10^{-2}$ , are moderately stripped,  $R_{str}/R_d \approx 0.6$ , at intermediate distances,  $0.5 < s_{orbit} < 1$ , from the cluster center and severely stripped closer to the cluster center. Satellites with lower  $M_{v,sat}/M_{v,gr}$  are severely stripped even at intermediate distances. Strip-

ping also occurs in groups. However, the same degree of stripping occurs for lower  $M_{v,sat}/M_{v,gr}$  in groups than in clusters. Dwarf galaxies are moderately to severely stripped at intermediate distances in groups, and large spiral galaxies can be moderately stripped if they travel to small  $s_{orbit}$ .

The model is simple and motivated by observations. Dark matter profiles are well matched to NFW profiles outside a possible core, observations of X-ray gas in clusters can be fit using  $\beta$  profiles, and the average gravitational potential of most galaxies should be well matched by the model potential. The model has a large number of parameters, but the values for many can be taken from observations. However, the model assumes that clusters are static. From an evolutionary standpoint, it is only valid after the group or cluster has acquired an ICM. On the other hand, in dynamic clusters bulk ICM motions may cause more stripping to occur than is predicted by the model. This is observed in the Virgo cluster (Kenney et al. 2004b).

Ram pressure stripping is not the only way to remove gas from galaxies. In groups and clusters tidal stripping of both gas and stars can occur (e.g., (Bureau et al. 2004; Patterson & Thuan 1992)). For dwarf galaxies it has been proposed that supernova winds associated with bursts of star formation may expel gas (Ferrara & Tolstoy 2000; Silich & Tenorio-Tagle 2001), and the efficiency of this mechanism may depend on the environment (Murakami & Babul 1999). However, ram pressure stripping is capable of removing gas from galaxies across a large range of galaxy masses and environments. In particular ram pressure stripping can act when supernova-driven ejection is likely to be inefficient and can remove gas from galaxies that are either not tidally interacting or that are experiencing only weak tidal interactions.

The tidal radius,  $r_t$ , at the physical orbital radius,  $r_{orbit}$ , as estimated using  $r_t = (M_{v,sat}/3M_{enc})r_{orbit}$ , can be compared to the stripping radius,  $R_{str}$ , as determined using the model. Here  $M_{enc}$  is the cluster mass enclosed within  $r_{orbit}$ . In scaled coordinates,  $r_t/R_d = \lambda_g s_{orbit} [3m(s_{orbit})]^{-1/3}$ , where  $m(s_{orbit}) = M_{enc}/M_{v,gr}$ . The H I fraction lost to tidal stripping depends only on the scaled size of the gas disk and  $s_{orbit}$  and not on either mass. Because the gas disk resides in the center of the satellite's dark halo, tidal stripping rarely effects the H I disk and practically never competes with the effect RPS. For example, in order for the H I disk to be tidally stripped to  $r_t/R_g = .8$ , a satellite must travel to  $s_{orbit} \approx .1$ . By this  $s_{orbit}$  the entire outer H I disk has been ram pressure stripped for almost all satellites.

The effect of varying the model's parameters was studied both to identify the parameters that most effect the extent to which an individual galaxy is stripped and to determine the range of satellite and cluster masses that result in the same  $R_{str}$ . The extent to which an individual galaxy is stripped depends most strongly on the galaxy's  $s_{orbit}$  or  $s_0$ , inclination,  $i$ , and disk scale length,  $\lambda_g$ , and on the cluster's ICM profile. Galaxies that reach smaller  $s_{orbit}$ , are face-on to the wind, have denser disks, or orbit through a denser ICM are more effectively stripped. Galaxies in the same cluster with  $M_{v,sat}$  that differ by as much as a factor of 25 can be

stripped to the same  $R_{str}$ . In different clusters, galaxies on identical orbits with identical morphologies, identical  $m_i$ ,  $\lambda_i$ ,  $c_s$ , can be stripped to the same  $R_{str}$  with  $M_{v,sat}$  values that differ by as much as a factor of 30.

Ram pressure stripping of satellite galaxies' outer gas disks and hot galactic halos is occurring frequently in both groups and clusters. In general, removing gas from a galaxy reduces star formation. The gas in the outer disk and hot galactic halo is not currently involved in star formation, but may feed future star formation if it is not stripped. Therefore, it would be interesting to study in more detail how the removal of this gas affects galaxy evolution and to determine if, to what extent, and how quickly star formation declines after a galaxy is stripped.

## 7. ACKNOWLEDGEMENTS

This project was advised by D. N. Spergel and funded by NASA Grant Award #NNG04GK55G. I'd like to thank the anonymous referee for useful comments.

## REFERENCES

Abadi, M. G., Moore, B. & Bower, R. G. 1999, MNRAS, 308, 947, astro-ph/9903436

Binney, J. & Merrifield M. 1998, Galactic Astronomy (Princeton: Princeton Univ. Press)

Binney, J. & Tremaine, S. 1988, Galactic Dynamics (Princeton: Princeton Univ. Press)

Blitz, L. & Robishaw, T. 2000, ApJ, 541, 675, astro-ph/0001142

Bravo-Alfaro, H., Cayatte, V., van Gorkom, J. & Balkowski, C. 2000, AJ 119, 580

Bullock, J. S., Kolatt, T. S., Sigad, Y., Somerville, R. S., Kravtsov, A. V., Klypin, A. A., Primack, J. R. & Dekel, A. 2001, MNRAS, 321, 559

Bureau, M., Walter, F., van Gorkom, J. & Carignan, C. 2004, in IAU Symp., 217, Recycling Intergalactic and Interstellar Matter, ed. P.-A. Duc, J. Braine, & E. Brinks (San Fransisco: ASP), 452, astro-ph/0311539

Cayatte, V., Kotanyi, C., Balkowski, C. & van Gorkom, J. H. 1994, AJ, 107, 1003C

Cole, S. & Lacey, C., 1996, MNRAS, 281, 716C, astro-ph/9510147v2

Ferrara, A. & Tolstoy, E. 2000, MNRAS, 313, 291,

Gavazzi, G., Boselli, A., Cortese, L., Arosio, I., Gallazzi, A., Pedotti, P., & Carrasco, L. 2006, A&A, 446, 839

Gill, S. P. D., Knebe, A., Gibson, B. K., & Dopita, M. A. 2004, MNRAS 351, 410

Giovanelli, R., & Haynes, M. P. 1983, AJ, 88, 881G

Gomez, P. L., et al. 2003, ApJ, 584, 210

Goto, T., Yamauchi, C., Fujita, Y., Okamura, S., Sekiguchi, M., Smail, I., Bernardi, M., & Gomez, P. L. 2003, MNRAS, 346, 601G, astro-ph/0312043

Grebel, E. K. 2002, in IAP Colloq. 17, Gaseous Matter In Galaxies And Intergalactic Space, ed. R. Ferlet, M. Lemoine, J.-M. Desert, & B. Raban (Paris: Frontier Group), 171, astro-ph/0110471

Gunn, J. E. & Gott, J. R. 1972, ApJ 176, 1

Helsdon, S. F. & Ponman, T. J. 2000, MNRAS, 315, 356

Hernquist, L., 1990, ApJ, 356, 359

Hogg, D. W. et. al. 2003, ApJ, 585, L5

Hogg, D. W. et al. 2003, ApJ, 601, L29

Johnston, K. V., Spergel, D. N., & Hernquist, L. 1995, ApJ, 451, 598

Kenney, J. D. P., Crowl, H., van Gorkom, J. & Vollmer, B. 2004, in IAU Symp., 217, Recycling Intergalactic and Interstellar Matter, ed. P.-A. Duc, J. Braine, & E. Brinks (San Fransisco: ASP), 217, 370

Kenney, J. D. P. & Koopmann, R. A. 1999, AJ, 117, 181K

Kenney, J. D. P., van Gorkom, J., Vollmer, B. 2004, AJ, 127, 3361K

Lokas, E. W. & Mamon, G. A. 2001, MNRAS, 321, 155, astro-ph/0002395

Marcolini, A., Brighenti, F., & D'Ercole, A. 2003, MNRAS, 345, 1329, astro-ph/0309026

Matthews, L. D. & Gallagher, J. S. 1997, AJ, 114, 1899

Miyamoto, M. & Nagai, R. 1975, PASJ, 27, 533

Mo, H. J., Mao, S., & White, S. D. M. 1998, MNRAS, 295, 319, astro-ph/9707093

Mohr, J. J., Mathiesen, B., Evrard, A. E. 1999, ApJ, 517, 627

Mori, M., Burkert, A. 2000, ApJ, 538, 559M, astro-ph/0001422

Murakami, I., Babul, A. 1999, MNRAS, 309, 161M

Navarro, J. F., Frenk, C. S., & White, S. D. M. 1997, ApJ, 490, 493

Osmond, J. P. F. & Ponman, T. J. 2004, MNRAS, 350, 1511

Patterson, R. J. & Thuan, T. X. 1992, ApJ, 400, L55

Popesso, P., Biviano, A., Bhooringer, H., Romaniello, M., & Voges, W. 2005, A&A, 433, 431P

Quilis, V., Moore, B., & Bower, R. 2000, Science 288, 1617

Roediger, E. Hensler, G. 2005, A&A, 433, 875R

Sanderson, A. J. R. & Ponman, T. J. 2003, in Clusters of Galaxies: Probes of Cosmological Structure and Galaxy Evolution, ed. J. S. Mulchaey, A. Dressler, & A. Oemler (Pasadena: Carnegie Observatories), 50, astro-ph/0303374

Sanderson, A. J. R., Ponman, T. J., Finoguenov, A., Lloyd-Davies, E. J., & Markevitch, M. 2003, MNRAS, 340, 989

Schulz, S. & Struck, C. 2001, MNRAS, 328, 185

Silich, S. & Tenorio-Tagle, G. 2001, ApJ, 552, 91, astro-ph/0101317

Solanès, J. M., Manrique, A., Garcia-Gomez, C., Gonzalez-Casado, G., Giovanelli, R. & Haynes, M. P. 2001, ApJ, 548, 97

Swaters, R. A., van Albada, T. S., van der Hulst, J. M., & Sancisi, R. 2002, A&A, 390, 829, astro-ph/0204525

Vitvitska, M., Klypin, A. A., Kravtsov, A. V., Wechsler, R. H., Primack, J. R., & Bullock, J. S. 2002, ApJ, 581, 799, astro-ph/0105349

Vollmer, B., Marcellin, M., Amram, P., Balkowski, C., Cayatte, V., & Garrido, O. 2000, A&A, 364, 532V

Vollmer, B., Balkowski, C., Cayatte, V., van Driel W. & Huchtmeier, W. 2004, A&A, 419, 35V

## APPENDIX

## A. NFW PROFILE

When simulations are run that allow cold, non-interacting particles to evolve gravitationally from a flat power spectrum at high redshift, the dark matter halos that emerge at low  $z$  are well fit by a universal density profile over many orders of magnitude in mass. This profile was originally parameterized by Navarro et al. (1997). Both the satellite and group/cluster dark matter halos are described using an NFW profile, the relevant properties of which are summarized here.

The NFW profile is

$$\frac{\rho(r)}{\rho_c^0} = \frac{\delta_{char}}{(r/r_s)(1+r/r_s)^2} \quad (A1)$$

where  $\rho_c^0$  is the average density of the universe at  $z = 0$ ,  $r_s$  is an inner scale radius, and  $\delta_{char}$  is a characteristic over-density. It can be rewritten in terms of a concentration,  $c$ , an overdensity,  $v_\rho$ , and a scaled radius,  $s \equiv r/r_v$

$$\frac{\rho(s)}{\rho_c^0} = \frac{v_\rho c^2 g(c)}{3s(1+cs)^2} \quad (A2)$$

$$c \equiv \frac{r_v}{r_s} \quad (A3)$$

$$\delta_{char} = \frac{v_\rho c^3 g(c)}{3} \quad (A4)$$

$$g(c) = \frac{1}{\ln(1+c) - c/(1+c)} \quad (A5)$$

The overdensity, virial mass,  $M_v$ , and virial radius,  $r_v$ , are related by

$$M_v = \frac{4}{3}\pi r_v^3 v_\rho \rho_c^0 \quad (\text{A6})$$

Note that the virial radius scales as  $M_v^{1/3}$ . The mass contained within  $s$  is

$$M(s) = g(c)M_v \left[ \ln(1 + cs) - \frac{cs}{1 + cs} \right] \quad (\text{A7})$$

and the gravitational potential is

$$\Phi(s) = -\frac{GM_v g(c)}{r_v} \frac{\ln(1 + cs)}{s} \quad (\text{A8})$$

The above can be found in (Cole & Lacey 1996; Lokas & Mamon 2001) and (Navarro et al. 1997).

## B. ORBITS IN AN NFW POTENTIAL

Bound orbits in a central force field travel between two radial extremes. These are found by solving.

$$\frac{1}{r^2} = \frac{2[\epsilon - \Phi(r)]}{l^2} \quad (\text{B1})$$

where  $\epsilon$  and  $l$  are the energy and angular momentum per unit mass (Binney & Tremaine 1988).

The scaled radial extremes,  $s_0$ , for an NFW profile are given by

$$\frac{1}{s_0^2} = \frac{-2}{b_s^2} \left[ 1 - \frac{\epsilon_v}{\epsilon} g(c) \frac{\ln(1 + cs_0)}{s_0} \right] \quad (\text{B2})$$

where  $\epsilon_v$  and  $b_s$  are defined as

$$\epsilon_v \equiv -\frac{GM_v}{r_v} \quad (\text{B3})$$

$$b_s^2 \equiv \frac{l^2}{|\epsilon|r_v^2} = \frac{b^2}{r_v^2} \quad (\text{B4})$$

The parameter  $b$  would be the impact parameter for an unbound orbit.

Conserving angular momentum and using Eq. B2, the orbital speed at the pericenter,  $v_0$ , is

$$v_0^2 = \frac{b_s^2}{s_0^2} \frac{\epsilon}{\epsilon_v} \frac{GM_v}{r_v} \quad (\text{B5})$$

It is proportional to  $M_v^{1/3}$  and depends on the concentration through  $s_0(c)$ .

At any point in the orbit, the orbital speed,  $v_{sat}$ , is

$$v_{sat}^2 = \frac{2GM_v}{r_v} \left[ g(c) \frac{\ln(1 + cs)}{s} - \frac{\epsilon}{\epsilon_v} \right] \quad (\text{B6})$$

## C. HOT GALACTIC HALO

The virial temperature,  $T_v$ , of a gravitational potential is defined by

$$\frac{3k_B T_v}{\mu m_p} \equiv \langle v^2 \rangle = \frac{|W|}{M_v} \quad (\text{C1})$$

where  $W$  is the work done by gravity in forming the halo,  $k_B$  is the Boltzmann constant,  $m_p$  is the mass of the proton, and  $\mu$  is the mean molecular weight (Binney & Tremaine 1988).

Using eqs. A2, A6, and A7, the virial temperature of an NFW profile is

$$\frac{|W|}{M_v} = \frac{GM_v}{r_v} c^2 g^2(c) \int_0^1 \frac{\ln(1 + cs) - cs/(1 + cs)}{s(1 + cs)^2} s ds \quad (\text{C2})$$

$$\equiv \frac{GM_v}{r_v} c^2 g(c) I_1(c) \quad (\text{C3})$$

A dimensionless temperature,  $t$ , is defined.

$$t(c) \equiv \left( \frac{k_B T_v}{\mu m_p} \right) \left( \frac{r_v}{GM_v} \right) \quad (\text{C4})$$

$$t(c) = \left( \frac{c^2 g(c) I_1(c)}{3} \right) \quad (\text{C5})$$

TABLE C1  
PARAMETER VALUES AND SCATTER

parameter	ref in text	reference model	mid mass model	low mass model	scatter	$\Delta P$ <sup>a</sup>	$\Delta M$ <sup>a</sup>
$\alpha$	Eq. 4	6.5	5.5	20	$\times 6$	6	15
$\beta^b$	Eq. 4	0.67	—	—	$\pm .08$	2	3
—	—	—	0.57	—	—	—	—
—	—	—	—	0.45	$\pm .08$	7.4	20
$r_{v,gr}/r_c^b$	Eq. 4	12	—	—	7 - 20	6	16
—	—	—	25	—	—	—	—
—	—	—	—	170	75 - 270	5.4	13
$i$	sec. 4.3	$0^\circ$	—	—	$0^\circ - 90^\circ$	4.5	10
$v_{sat}(s_{orbit} = 1)/v_c$	Eq. B6	1.15	—	—	$\pm .6$	1.4	1.6
$c_g$	Eq. 2	5.5	7.5	10	5-16	1.1	1.2
$c_s$	Eq. 9	12	—	20	12-20	1.4	1.7
$\lambda_g$	Eq. 11	5.7	—	—	$\pm 1.4$	8	20
$\lambda_d/\lambda_g$	Eq. 6	6	—	—	$\pm 2.5$	1.2	1.4
$\lambda_h$	Eq. 6	0.04	—	—	—	—	—
$\lambda_b$	Eq. 8	180	—	na	—	—	—
$m_{dg}$	Eq. 11	0.008	—	0.016	$\times 1.5$	1.5	1.8
$m_{ds} + m_{H_2}$	Eq. 6	0.05	—	0.04	$\pm .01$	1.3	1.4
$m_b$	Eq. 8	0.017	—	0	0.012-0.024	1.1	1.2
$m_{sg}$	Eq. 13	0.005	—	—	$\times 1.5$	1.5	1.8
$s_0$	Eq. B2	0.35	—	—	$\pm .12$	5.4	13

<sup>a</sup> $\Delta P$  and  $\Delta M$  columns list the scatter in  $P_{ram}$  or  $P_{rest}$  and  $M_{v,sat}/M_{v,gr}$ . The scatter is given as the fractional change when the parameter of interest is varied over its entire range. Therefore,  $\log(\Delta M) \approx 2\sigma_{log}(M_{v,sat}/M_{v,gr})$ .

<sup>b</sup>The first row shows affects of scatter for the large mass model and the third row for the small mass model. Columns 7 and 8 show the fractional increase in  $P_{ram}$  at  $s_{orbit} = 1$ .

For a gas in hydrostatic equilibrium in potential  $\phi$ , ignoring self-gravity

$$\rho(r) = \rho_0 \exp\left(\frac{\mu m_p}{k_B T} [\phi(r) - \phi(0)]\right) \quad (C6)$$

Combining eqs. C3 and C6, the gas density profile is

$$\rho_g(s) = \rho_0 \exp\left(\frac{3}{cI_1(c)} \left[ \frac{\ln(1+cs)}{cs} - 1 \right]\right) \quad (C7)$$

Letting the gas mass within  $r_v$  equal a fraction  $m_{sg}$  of the virial mass results in a central density of

$$\rho_0 = \frac{\rho_0^c v_\rho m_{sg}}{3I_2(c)} \quad (C8)$$

The integral,  $I_2(c)$ , is

$$I_2(c) = \int_\epsilon^1 s^2 ds \exp\left(\frac{3}{cI_1(c)} \left[ \frac{\ln(1+cs)}{cs} - 1 \right]\right) \quad (C9)$$

The scaled density profile  $j$  is defined by

$$j(s, c) \equiv \frac{1}{I_2(c)} \exp\left(\frac{3}{cI_1(c)} \left[ \frac{\ln(cs)}{cs} - 1 \right]\right) \quad (C10)$$

$$\rho(s) = \left(\frac{v_\rho \rho_0^c}{3}\right) m_{sg} j(s, c) \quad (C11)$$